Damping and Structural Control of the JPL Phase 0 Testbed Structure

Published: *Journal of Intelligent Material Systems and Structures,* vol. 2, No. 3, pp. 281–300, July, 1991.
doi: 10.1177/1045389X9100200303

Damping and Structural Control of the JPL Phase 0 Testbed Structure*

James L. Fanson, Cheng-Chih Chu and Boris J. Lurie

Jet Propulsion Laboratory
California Institute of Technology
4800 Oak Grove Drive
Pasadena, CA 91109

Roy S. Smith

Department of Electrical and Computer Engineering
University of California at Santa Barbara
Santa Barbara, CA 93106

Abstract

This paper describes recent advances in structural quieting technology as applied to active truss structures intended for high precision space based optics applications. The active structure incorporates piezoelectric active members which exert control forces internal to the structure and thereby improve the structure's dimensional stability. The control architecture involves two layers of feedback control. The first utilizes collocated measurements of force and velocity at the active member to achieve active damping, the second utilizes noncollocated measurements of acceleration at the location of a simulated optical component to achieve structural stabilization. The local control loops are based on the concept of impedance matching, the global control loops are designed using robust control methods. These two levels of control are intended to operate simultaneously; however, in this paper each approach is applied individually. The combined implementation is left for future work.

Introduction

THE Jet Propulsion Laboratory has embarked on a program to develop the technology to achieve submicron level dimensional stability on large complex optical class spacecraft. The focus mission for this work is an orbiting interferometer telescope [1]. A series of evolutionary testbed structures are being constructed for the purpose of developing and demonstrating the technology required for such a mission. The Phase 0 testbed structure has been dedicated to the development of active structure

*This paper was presented at the First Joint U.S./Japan Conference on Adaptive Structures, Maui, Hawaii, November 13–15, 1990.

hardware and feedback control methodologies, its configuration is described in detail elsewhere [2].

The top level architecture for achieving submicron stability involves a layering of technologies including active vibration isolation, structural quieting, and active optical compensation [3]. This paper describes recent advances in the structural quieting area. By structural quieting, we mean that the structural portion of the spacecraft is designed so as not to deform or vibrate at locations, in directions, or over frequency ranges that adversely affect the overall performance of the spacecraft. Our approach to this objective involves the use of passive damping, active damping, and active structural stabilization. Passive and active damping have the effect of reducing vibration at all points of the structure by preventing modal resonances from building up to large amplitude.

Active damping is achieved by making each active member simulate a passive damping device over a specified frequency range. In this respect, all active members work independently of each other. Structural stabilization is intended to take over where damping leaves off, by making all active members work in concert to remove any residual motion at locations and in directions that impair performance. The active damping problem is a collocated single input problem, meaning that certain special properties of the structure enable controller designs that are very robust against uncertainty in the plant. In fact, minimal knowledge of the plant is required to achieve good damping performance.

The stabilization problem is more difficult because it involves multiple inputs and noncollocated measurements. An accurate mathematical model of the plant between inputs (control and disturbance) and outputs is required. Accurate models of lightly damped structures are problematical because small perturbations in parameters can lead to large input/output errors. Robust control methods ($\mathcal{H}_\infty$ and μ-synthesis) have been developed to enable the design of multivariable controllers that will perform on systems that are uncertain [4]. These paradigms require that the designer not only supply a model of the physical system, but also an explicit measure of the uncertainty. This approach therefore involves producing good multivariable models (system identification) and estimating appropriate levels of uncertainty in addition to synthesizing the controllers. Our experiments are designed to explore the applicability of these methods to the structural control problem, starting with lightly damped structures and progressing to the more heavily damped.

The first portion of the paper describes the active damping controller, the second portion describes the stabilization controller, and the final portion describes the system identification approach we have followed to produce multivariable models. We close with a discussion of the results and thoughts for future research.

Local Controllers—Active Damping

Damping is the most effective means of reducing vibration in an otherwise lightly damped structure. Passive dampers, such as fluid dashpots, dissipate energy by causing the dual power quantities of force and velocity to be in phase locally at the damper. Optimal damping performance is achieved by matching the impedance of the damper to the structure. The mechanical model for a linear viscous damper is shown in Figure 1, where the damping mechanism is represented by a dashpot with damping coefficient c that is elastically coupled to the structure by the spring k_2, and

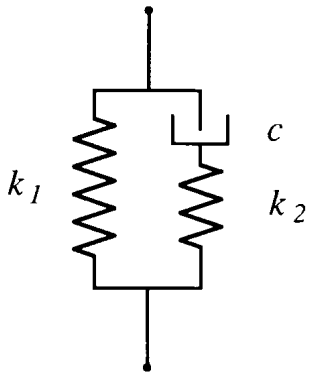

Figure 1: Elastically coupled viscous damper.

shunted by the spring k_1. By selecting the values of c, k_1, and k_2, the impedance of the damper can be matched to the structure over some frequency range.

An analogous approach can be taken with the active member, i.e., the active member can be made to emulate the passive damper of Figure 1 by appropriate feedback of collocated force and velocity. As it happens, the primary source of impedance mismatch between a structural element of a typical truss and the driving point impedance of the remainder of the structure is the stiffness mismatch. Unless the individual member is softened significantly, heavy damping cannot generally be achieved. We have found that local force feedback, accompanied by small phase shift, can achieve nearly optimal damping performance. A more sophisticated approach involves feedback of both force and velocity (obtained by differentiating displacement) through a bridge feedback circuit [5]. Bridge feedback is a standard technique in amplifier design for enforcing the input or output impedance of an amplifier by feeding back both voltage and current (the electrical dual power quantities). The mechanical case is strictly analogous.

Our implementation exactly parallels the mechanical scheme depicted in Figure 1. An analog bridge feedback circuit has been designed with three dials corresponding to c, k_1, and k_2, such that the engineer need only measure the input impedance of the structure and then adjust the dials to the desired setting for an optimal impedance match. The required impedance measurement is easily obtained by exciting the structure using the active member and measuring the resulting ratio of force to velocity at the member. This dial-a-strut controller can be adjusted to a wide range of parameter values allowing for great flexibility. The details of the design of the dial-a-strut controller will be presented in a future report.

Figure 2 shows an example of damping performance for one and two active members located in longerons of the testbed structure. The resonance peak at 11.5 Hz corresponds to a torsional mode that does not involve strong participation of the two longerons used in the test, which is why the damping in this mode is less than that for the two bending modes. Figure 3 shows the damping performance for a crude tuning of force feedback alone. The force feedback scheme provides somewhat more phase margin than the bridge feedback, but somewhat less optimal performance. One additional benefit of the bridge feedback approach is that the impedance enforced by the feedback is indepedant of the shape of the loop transmission function, so long as the gain is sufficiently high. This means that the loop shape can be designed to satisfy other objectives (for example, structural stabilization).

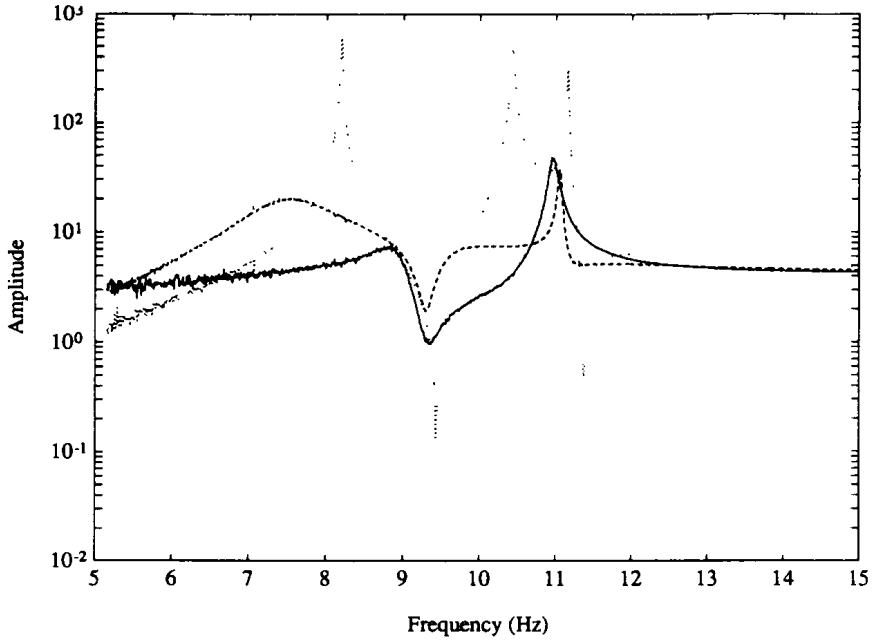

Figure 2: Transfer function between disturbance input and z-accelerometer output for open loop plant (dotted), one dial-a-strut with bridge feedback (dashed), and two dial-a-struts with bridge feedback (solid).

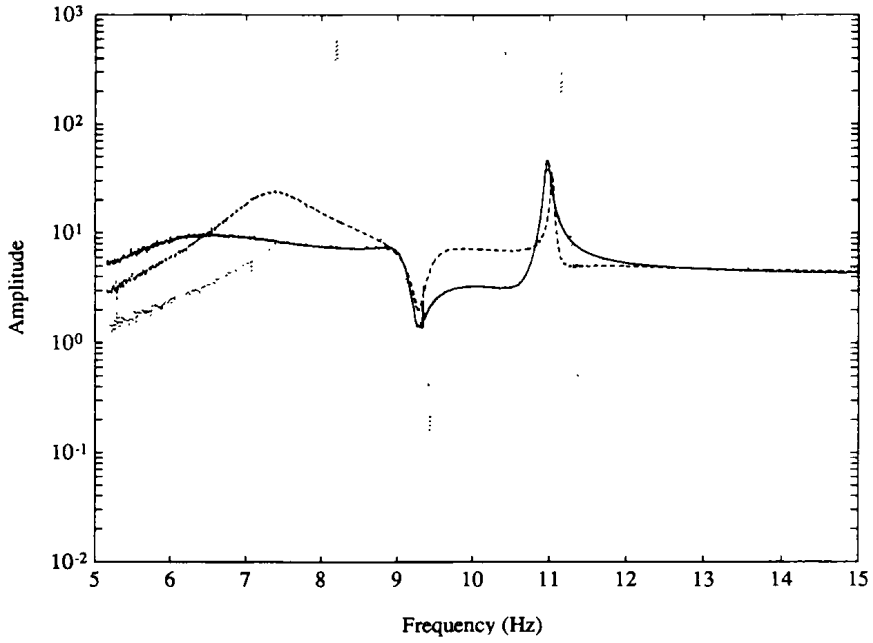

Figure 3: Transfer function between disturbance input and z-accelerometer output for open loop plant (dotted), one dial-a-strut with force feedback (dashed), and two dial-a-struts with force feedback (solid).

Structural Stabilization

The structural stabilization loop is intended to be closed around the local active damping loops to provide additional stabilization to specific measures of performance—line of sight, for example—that cannot be achieved by damping alone. In these experiments, however, the outer loops are designed without the damping loops present. This leads to a lightly damped structure that presents a worst case plant for which to design robust controllers. In order to assess the effect of damping on the design process, a passive damper is placed in one of the nonactive members of the truss, which increases the damping in the lower three modes from about 0.1 percent of critical to about 1.0 percent of critical.

The primary challenges in designing the outer loops are: (1) to obtain an accurate mathematical model that relates inputs from the disturbances and actuators to the outputs from the sensors, and (2) to parameterize the uncertainty in the model in a way that is both physically meaningful and mathematically tractable [3]. In early experiments, we relied on a finite element model of the structure to provide the mode shapes used in the state space model, and used measured values of modal frequency and damping. Even though the finite element model was considered well-correlated from a structural engineering standpoint, our experience on this structure indicated that with damping on the order of 0.1 percent of critical, it was not possible to obtain a sufficiently accurate plant model for control design [3]. We therefore began using models based on input/output measurements from the physical system. Our ad-hoc approach to this system identification problem is outlined in the last section of the paper.

The block diagram used for control design is shown in Figure 4. This is the same interconnection structure that was used for the designs based on the finite element models. The inputs and outputs are normalized by means of frequency domain weighting functions such as those shown in Figure 5. The plant uncertainty is parameterized by means of two full block perturbations Δ_a and Δ_m; additive and output multiplicative blocks, respectively. Different designs are obtained by manipulating the weights. While this simple scheme for parameterizing uncertainty is not necessarily the best for lightly damped structures, it serves as a starting point and basis for comparison.

The controllers were designed to minimize the response in three directions of a point at the top of the structure, using measurements from three accelerometers at the top location, and using three active members at the base of the truss as shown in Figure 6. No collocated measurements were used. The modes of the structure are divided into two groups, the first group near 10 Hz, and the higher group starting at approximately 30 Hz. The higher modes involve significant bending of the truss members, and are therefore only marginally controllable from the location of the active members. Performance was requested for the lower modes only, the loop gain diminishing rapidly after 11 Hz. All algorithms were implemented on the HUGH 9000 real time control computer at an update rate of 1000 samples per second [6]. The number of controller states varied from 28 to 35.

Two controllers were designed for the undamped structure. The first, K_1, is a nonaggressive design that achieved gain stabilization in the higher modes, that is, the loop transmission function is less than one for the higher frequency modes. The second controller, K_2, is a more aggressive design that resulted from significantly

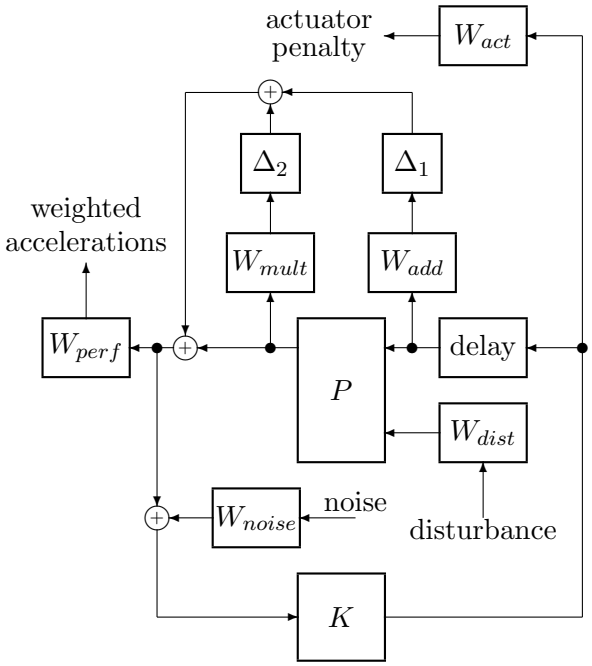

Figure 4: Interconnection structure for control design. P is the multi-input plant model, K is the controller.

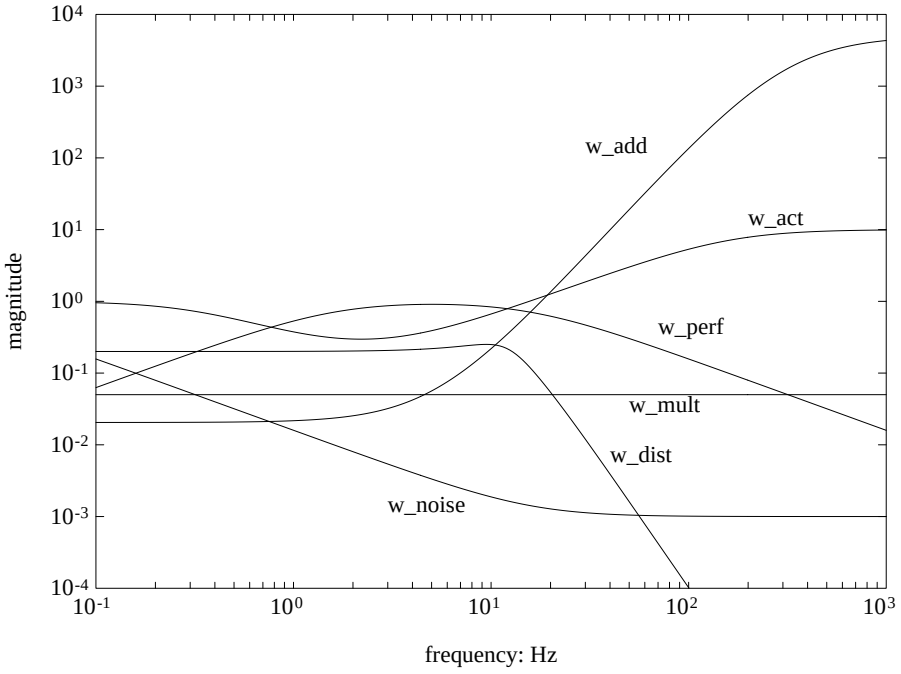

Figure 5: Weighting functions used in the design of controller K_2.

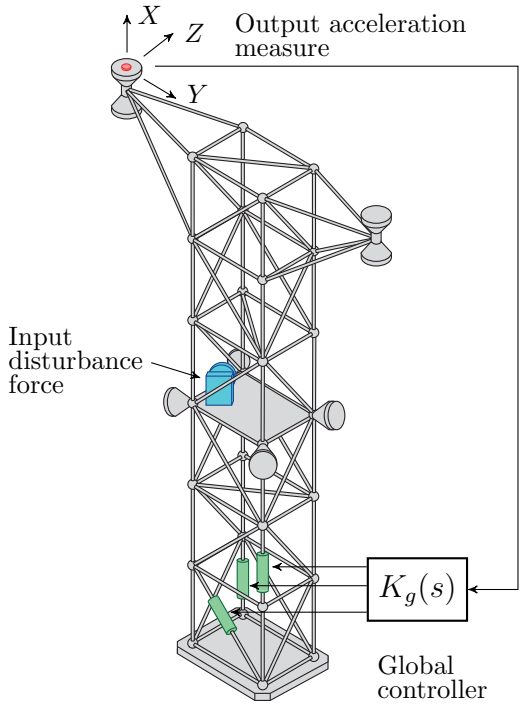

Figure 6: Location of sensors and actuators for noncollocated controllers.

lowering the additive uncertainty weight associated with the higher frequency modes. Figure 7 shows the loop transmission function for this case, and several of the higher modes are seen to peak above the 0 db line.

Figure 8 shows the actual closed loop performance measured between the disturbance input and the z-accelerometer output for controller K_2. Overplotted are the closed loop predictions based on the actual measured open loop plant transfer function, and based on the nominal plant model (uncertainty weights set to zero). The first observation is that the two predictions do not coincide, a result of the fact that the reduced order identified model is in error to some degree. In the case of the undamped structure, a local mode from the disturbance shaker was not included in the model with the result that the transfer functions from the disturbance input were not well represented. This was corrected in the model of the damped structure. The second observation is that the prediction based on the measured open loop transfer function differs only slightly from the actual measured closed loop performance.

The effect of feedback on performance is shown in Figure 9. Frequency response functions from disturbance force input to z-accelerometer output are plotted for the open loop case and for both controllers K_1 and K_2. As expected, design K_2 results in superior performance. A very weak instability was observed with design K_2 near 33 Hz, which was seen only in the x-accelerometer output. This is the first high frequency mode which is not gain stabilized (see Figure 7).

To determine the effect of damping on the closed loop performance, a D-strut passive damper was installed in the truss to add a small amount of damping to the lower modes. The higher modes were largely unaffected. Controllers K_3 and K_4 were designed with similar weighting functions as the previous cases, but were both designed with gain stabilized higher modes. Figure 10 compares the measured and predicted closed loop performance for design K_4. The predictions based on measured

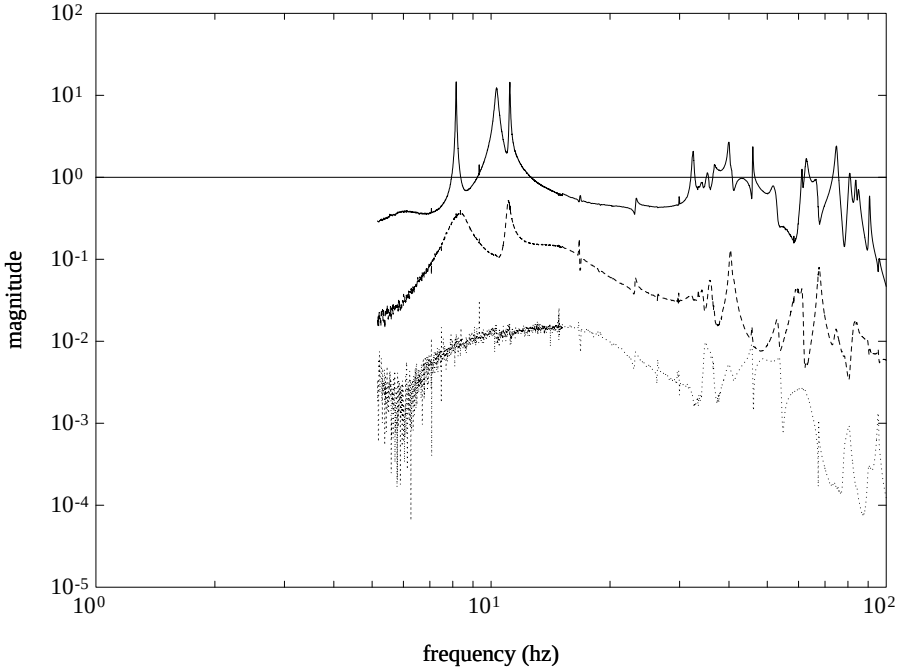

Figure 7: Loop gain for controller K_2 using measured plant data and analytical controller.

plant data and the nominal model agree much more closely in this case due to an improved identified model.

The closed loop performance on the damped plant is somewhat better than on the undamped plant in the second and third modes, and somewhat poorer in the first mode. These differences are more likely the result of different choices of weighting functions than on the passive damping level. On balance, the passive damping does not appear to have contributed significantly to the closed loop performance on the nominal system.

As a test of the robust performance characteristics of controller K_4 (designed for the damped structure), it was closed on the *undamped* structure. The system remained stable, and the performance on both plants is compared in Figure 12. Performance dropped by approximately a factor of two in the first and third modes, with no change in the second mode, even though the damping in the plant dropped by an order of magnitude. The robustness of the controllers to other forms of plant perturbation remains to be tested.

MIMO State-Space System Identification

A method for identifying a four-input, three-output state space realization of a nominal model for the precision truss is described. The inputs are the midbay shaker and the three active members, designated AM11, AM22, and AM101. The outputs are the X, Y, and Z accelerometers on outrigger 41. The required model, denoted by $P(s)$, is shown schematically in Figure 13.

The problem is considered only from an input-output point of view. The objective is the minimization of a least squares error in the input-output transfer functions. From the point of view of designing a controller, it is not necessary to use a modal

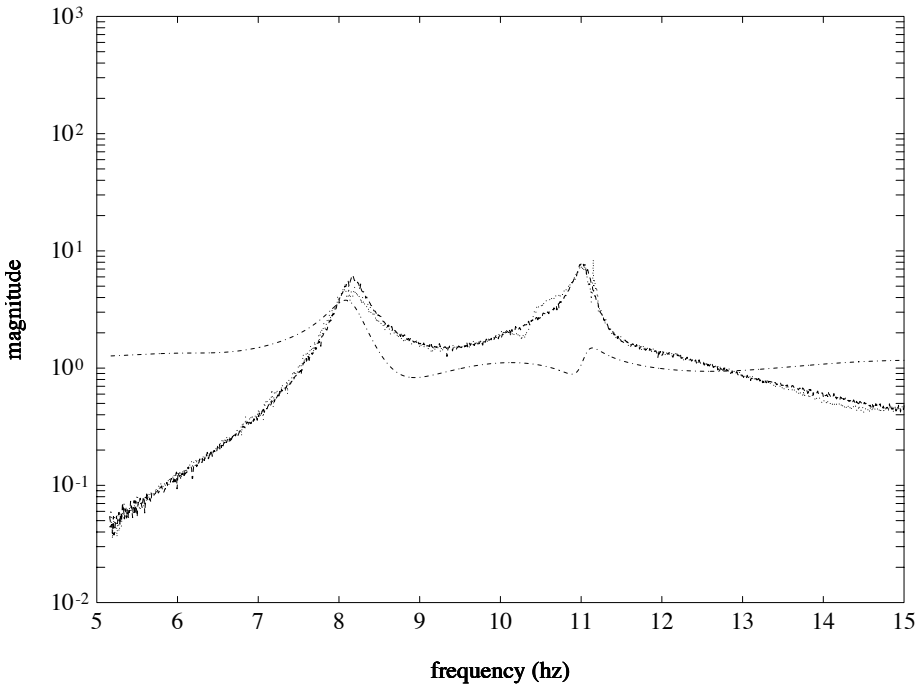

Figure 8: Closed loop performance for controller K_2. Dashed line is measured closed loop data. Dotted line is predicted based on measured open loop plant data. Dot-dashed line is predicted based on nominal plant model.

model. The model is used in a robust control design framework which also includes norm-bounded perturbations. This influences what is considered to be an acceptable model. For example, including an additive uncertainty of the form $P(s) + W(s)\Delta$, $\|\Delta\| \leq 1$, means that errors near the zeros of transfer function elements of $P(s)$ are not as significant as errors near the poles of $P(s)$—observed experimental errors can be attributed to a small perturbation, Δ, when the response of the system is already small.

For the identification approach used in this study, the desired model, $P(s)$ is assumed to have a state space representation given by

$$\begin{bmatrix} \dot{x} \\ y \end{bmatrix} = \begin{bmatrix} A & B \\ C & D \end{bmatrix} \begin{bmatrix} x \\ u \end{bmatrix}.$$

The corresponding transfer function is given by

$$P(s) = \left[C(sI - A)^{-1}B + D\right].$$

The procedures used assume that a frequency domain estimate of the input, $U(j\omega)$, and output signals, $Y(j\omega_i)$, are available at a finite number of frequencies, ω_i, $i = 1, \ldots, m$. The problem is then, find A, B, C, and D such that

$$Y(j\omega_i) = \left[C(j\omega_i I - A)^{-1}B + D\right] U(j\omega_i)$$

for $i = 1, \ldots, m$.

In general A, B, C, and D are overdetermined. The methods outlined here attempt to find the B, C, and D matrices such that the objective function

$$\left\{ \sum_{i=1}^{m} \|Y(j\omega_i) - P(j\omega_i)U(j\omega_i)\|^2 \right\}^{1/2},$$

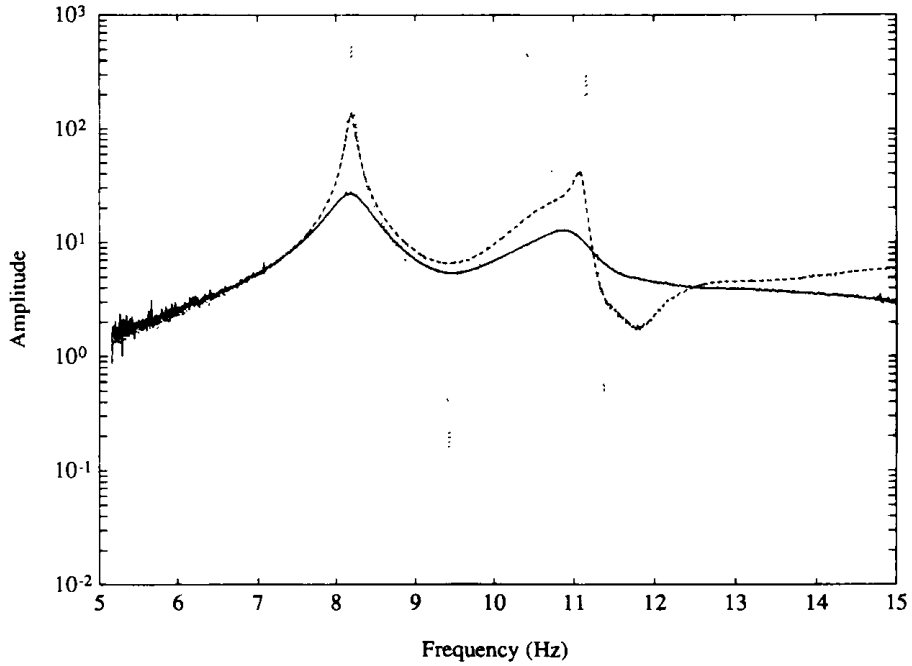

Figure 9: Comparison of open and closed loop performance for controllers K_1 and K_2.

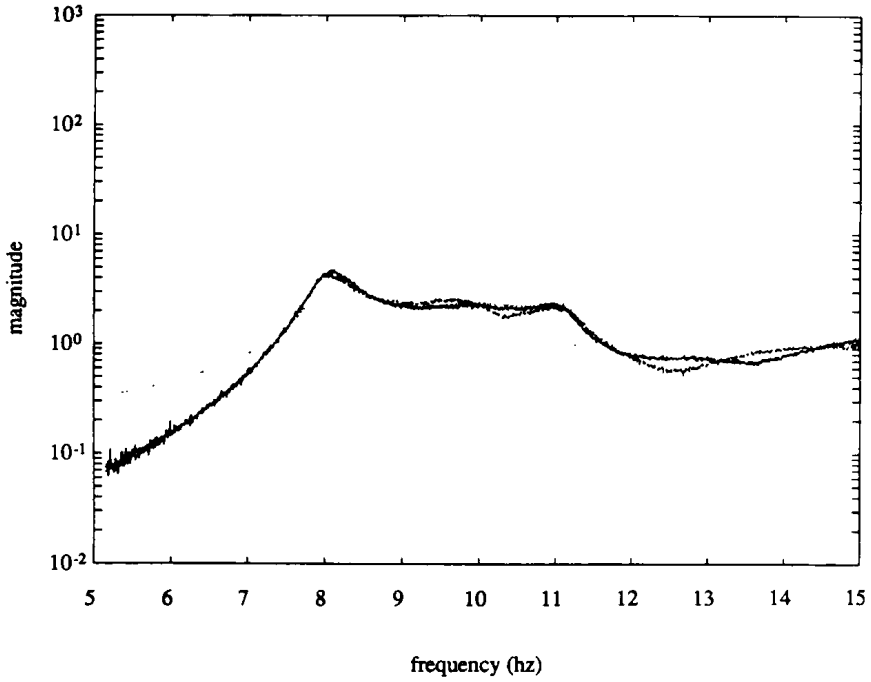

Figure 10: Closed loop performance for controller K_4. Solid line is measured closed loop data. Dashed line is predicted based on measured open loop plant data. Dotted line is predicted based on nominal plant model.

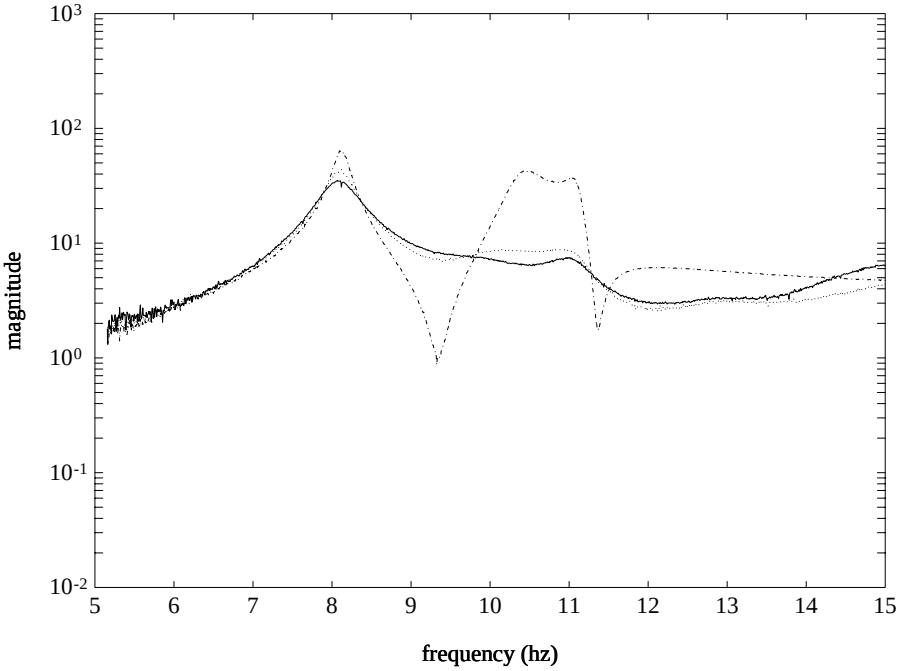

Figure 11: Comparison of open and closed loop performance for controllers K_3 and K_4 on passively damped structure.

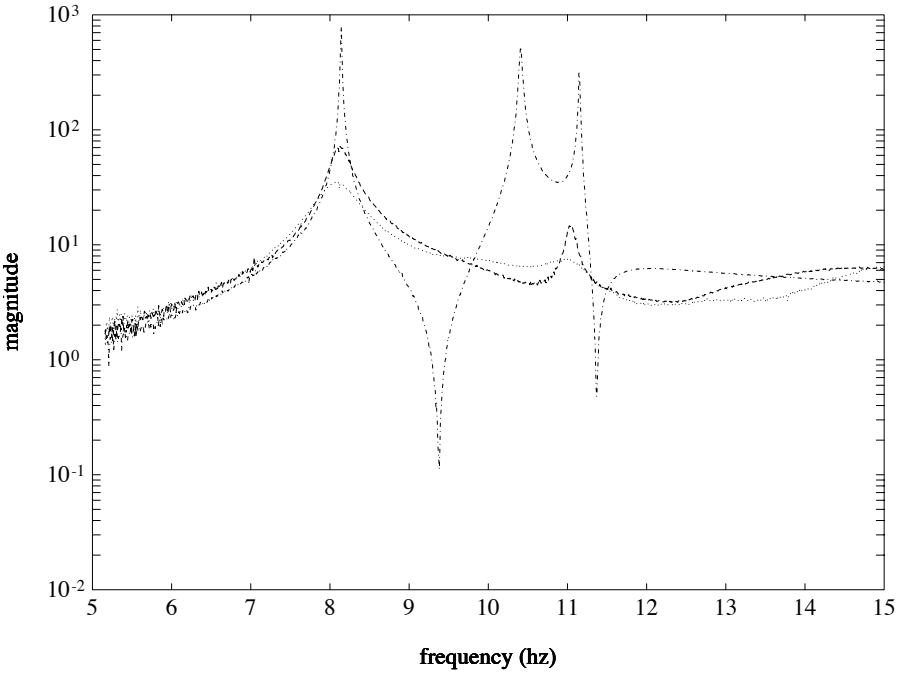

Figure 12: Dot-dashed line is undamped plant. Dotted line is controller K_4 closed on the damped structure. Dashed line is K_4 closed on the undamped structure.

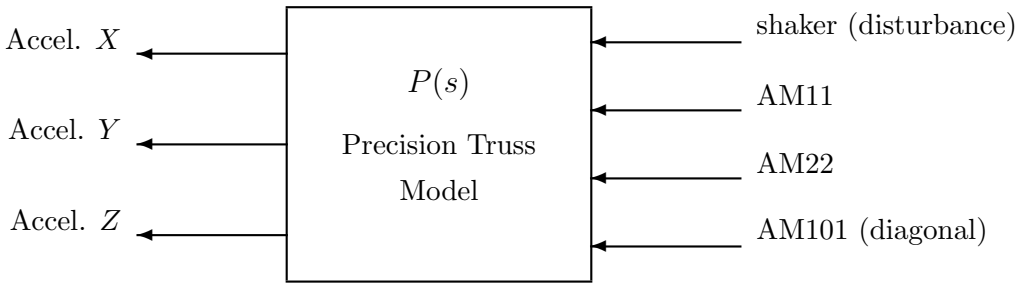

Figure 13: Schematic representation of precision truss model.

where $P(j\omega_i) = C(j\omega_i I - A)^{-1}B + D$, is minimized.

The approach is to choose an A matrix based on estimates of the frequency and damping of each mode, and then successively refine the B, C, and D matrices to minimize the above objective function. Estimating the A that minimizes the objective function is a nonlinear problem as A enters in the inverse term of the transfer function. However choosing the minimizing B, C, or D matrix is a linear least squares problem.

For example, consider the case of choosing the C to minimize the least square error between Y predicted from the known input, U, A, B, and D, and the observed Y. Define $Z(j\omega)$ by

$$Z(j\omega) = (j\omega I - A)^{-1}BU(j\omega),$$

then the ideal input-output relationship is,

$$Y(j\omega) - DU(j\omega) = CZ(j\omega).$$

This relationship must hold for each frequency, ω_i, $i = 1, \ldots, m$, for a single choice of C. Each of the m equations can be written as a column in a matrix equation, leading to the equivalent condition,

$$[Y(j\omega_1) \ldots Y(j\omega_m)] - D\,[U(j\omega_1) \ldots U(j\omega_m)] = C\,[Z(j\omega_1) \ldots Z(j\omega_m)]\,.$$

Finding the C to minimize,

$$\left\| \; [Y(j\omega_1) \ldots Y(j\omega_m)] - D\,[U(j\omega_1) \ldots U(j\omega_m)] - C\,[Z(j\omega_1) \ldots Z(j\omega_m)] \; \right\|,$$

or equivalently,

$$\left\{ \sum_{i=1}^{m} \|Y(j\omega_i) - P(j\omega_i)U(j\omega_i)\|^2 \right\}^{1/2},$$

is a linear least squares problem. The problem of choosing the minimizing B and D can be similarly formulated. This technique is applicable to multiple-input, multiple-output (MIMO) systems as the $Y(j\omega_i)$ and $U(j\omega_i)$ can be vectors. Complete descriptions of these algorithms are given in Reference [7].

The A matrix is estimated independently of the main iteration by considering each mode individually and estimating its frequency and damping. It should be noted that this is not a general procedure—it relies on the response being close to modal and the modes being separated.

The suggested method for obtaining a state-space model is therefore:

- Obtain frequency domain representations of the experimental input and output signals, $U(j\omega)$ and $Y(j\omega)$.
- Examine a SISO estimated transfer function and estimate modal frequencies and damping values. This gives an A matrix.
- Successively iterate on finding the best (in the above least squares sense) B, C, and D matrices to fit the experimental data.

An obvious improvement to the algorithm is to include a means of updating the A matrix (i.e., refining the modal frequency and damping values). This is a nonlinear optimization problem and was not found to be required for the precision truss experiment.

This method will allow arbitrary B, C, and D matrices and consequently will not, in general, yield a modal model of the system. However it does give a good input/output representation, and for the purpose of control design, this is sufficient. For the rest of this section, details of the identification experiment for the undamped structure will be presented.

A Tektronix 2630 Signal Analyzer, connected to an IBM PC, was used for the experiments. This is a complete acquisition/analysis system with one output and four input channels. Analysis software allows real time averaging of the FFT data. In the experiments outlined here the four channels were the excitation and the X, Y, and Z accelerations. Using this number of channels allows estimation of single-input, multiple-output (SIMO) transfer functions for each of the four inputs.

For each input zoom transforms were performed over the ranges 5 to 15 Hz and 10 to 110 Hz. 4096 point FFTs were calculated and averaged in real time resulting in 1600 points of the averaged estimated transfer function over each frequency range. These two frequency ranges were combined to give a single SIMO transfer function estimate for each of the four inputs. The data was decimated over certain frequency ranges to reduce the computational burden and introduce a frequency weighting for the least squares fitting. The three modes of greatest interest, those in the range 6.9 Hz to 12.0 Hz, were weighted the most strongly. The modes in the range 29 Hz to 38 Hz are also slightly emphasized in the weighting. After decimation, each SIMO transfer function estimate contained 982 frequency points.

For the system identification, only the eleven modes making the largest contribution to the response were chosen for inclusion in the model. Identifying the modal frequency and damping for each of these modes completely determines the A matrix.

The frequency and damping of each mode were identified by fitting a second order rational function to SISO data. Note that using four SIMO experiments gives twelve SISO transfer functions. Ideally, identical frequencies and dampings will appear on all transfer functions. In practice this was not the case, particularly on the transfer functions which have the shaker as an input. The shaker itself has a local mode close to 7 Hz. When not being driven, the shaker looks to the rest of the structure as a spring damper system. This gives slightly different modes when the shaker is being driven with the second mode of the structure (at 10.3 Hz) being affected the most.

In the final design model the midbay shaker is a disturbance input. The shaker transfer function can be viewed as a weighting function describing the relative affect of the disturbance on each of the modes. Accuracy in this weighting function is not critical to stability of the closed-loop system. For this reason the modes identified from the active member to acceleration transfer functions were used for the A matrix.

Fortunately there was very good agreement on the frequency and damping values for all of these modes.

Each preprocessed SIMO experimental data file contains three complex valued transfer function estimates. Conceptually, one can view this as a three by one vector at each frequency. Denote each SIMO transfer function estimate by $S_{.,k}(i) = S_{.,k}(j\omega_i)$, where k is the input (having values 1 to 4, corresponding to shaker, AM11, AM22, and AM101), and i is the frequency ($i = 1, \ldots, 982$). When referring to the transfer function for a particular output, the first index will be used with the X, Y, and Z accelerations being indices 1 to 3 respectively. Therefore a SISO transfer function estimate is denoted by $S_{l,k}(i)$, $l = 1, 2, 3$, $k = 1, 2, 3, 4$, $i = 1, \ldots, 982$. One can view the data as a matrix of SISO transfer function data,

$$\begin{bmatrix} \text{X accel.} \\ \text{Y accel.} \\ \text{Z accel.} \end{bmatrix} = \begin{bmatrix} S_{1,1}(i) & S_{1,2}(i) & S_{1,3}(i) & S_{1,4}(i) \\ S_{2,1}(i) & S_{2,2}(i) & S_{2,3}(i) & S_{2,4}(i) \\ S_{3,1}(i) & S_{3,2}(i) & S_{3,3}(i) & S_{3,4}(i) \end{bmatrix} \begin{bmatrix} \text{shaker} \\ \text{AM11} \\ \text{AM22} \\ \text{AM101} \end{bmatrix}.$$

The desired state space model for the system will be denoted by M, with $M_{l,k}$ referring to a particular input-output pair, and $M(i)$ referring to the transfer function value at frequency ω_i. The aim of the identification procedure is to generate A, B, C, and D, such that,

$$M(i) = C(j\omega_i I - A)^{-1}B + D, \quad i = 1, \ldots, 982,$$

and

$$M_{l,k}(i) \approx S_{l,k}(i), \quad l = 1, 2, 3, \quad k = 1, 2, 3, 4, \quad i = 1, \ldots, 982.$$

Each column of M, $M_{.,k}(i)$, was generated from the SIMO data. By defining, for each input, k, $Y(j\omega_i) \in \mathcal{C}^4$, and $U(j\omega_i) \in \mathcal{C}$, as follows,

$$Y(j\omega_i) = S_{.,k}(i), \quad U(j\omega_i) = 1, \quad i = 1, \ldots, 982,$$

the least squares techniques described previously produced models with transfer functions approximating the SIMO transfer function estimates. Essentially, the output is defined as the experimental transfer function data and the input is defined as unity. Note that this trick will not work with MIMO data.

Each SIMO model, $M_{.,k}$, $k = 1, 2, 3, 4$, was estimated using the algorithm described above. The resulting state space models are,

$$M_{.,k} = C_k(sI - A)^{-1}B_k + D_k, \quad k = 1, 2, 3, 4,$$

where $C_k \in \mathcal{R}^{3\times 22}$, $B_k \in \mathcal{R}^{22\times 1}$, $D_k \in \mathcal{R}^{3\times 1}$, and $A \in \mathcal{R}^{22\times 22}$. The A matrix contains the frequency and damping o the 11 modes (giving 22 states), and all models share this A matrix.

As the final model is linear one can generate a MIMO model by concatenating each SIMO model as follows,

$$M = \begin{bmatrix} M_{.,1} & M_{.,2} & M_{.,3} & M_{.,4} \end{bmatrix}.$$

M now has four inputs and three outputs, and $M_{l,k}(j\omega_i) \approx S_{l,k}(i)$, $l = 1, 2, 3$, $k = 1, 2, 3, 4$, and $i = 1, \ldots, 982$. However the state dimension has increased to 88 states.

Ideally, one would like a model containing only the 11 identified modes (22 states). To obtain this the following procedure was used.

- Concatenate each of the SIMO models to produce the 88 state MIMO model, M.
- Reduce the order of M to 22 states by balanced truncation.
- Create a fictitious MIMO problem to improve the least squares fit to the data.

The state space manipulations for concatenating the SIMO systems into a single MIMO system are well known. Similarly, balanced truncation is a well known means of model reduction. The balanced truncation procedures result in a 22 state model with significant errors. These can be reduced by MIMO least squares fitting to the data. The procedure for doing this is slightly different to that for the SIMO models.

Improving the B and D matrices is again a linear least squares problem. These can be done an input at a time for each of the SIMO transfer function estimates. The required B and D can be partitioned and considered as

$$B = \begin{bmatrix} B_1 & B_2 & B_3 & B_4 \end{bmatrix}, \quad B_k \in \mathcal{R}^{22\times 1} \quad \text{and} \quad D = \begin{bmatrix} D_1 & D_2 & D_3 & D_4 \end{bmatrix}, \quad D_k \in \mathcal{R}^{3\times 1}.$$

Now each B_k column is updated with the least squares technique by defining the input $U(j\omega_i) = 1$, and the output $Y(j\omega_i) = S_{.,k}(i)$. The C and A matrices used are those resulting from the balanced truncation. This procedure can also be used to update each column of the D matrix.

The procedure for updating the C matrix is now more complicated. One has to create a fictitious MIMO problem. This is done by defining the output, Y, as

$$Y(j\omega_i) = S_{.,1}(i) + jS_{.,2}(i) - S_{.,3}(i) - jS_{.,4}(i),$$

and the input, U, as

$$U(j\omega_i) = \begin{bmatrix} 1 \\ j \\ -1 \\ -j \end{bmatrix}$$

If the "true" system were linear this would be an input/output pair generated by the system. The multipliers, -1, j, and -j on the inputs and outputs were used in the hope of avoiding numerical problems. The previously described least squares technique is now used to update C. Note that this fictitious MIMO problem cannot be used to update the B and D matrices — a rank deficient least squares problem will result.

An iteration was set up to update the MIMO model using the above methods. Each step of the iteration can be summarized as,

- Update B_k, $k = 1, \ldots, 4$ from the SIMO transfer function estimates.
- Concatenate $B_1, \ldots, B_4$ to create an updated B.
- Update D_k, $k = 1, \ldots, 4$ from the SIMO transfer function estimates.
- Concatenate $D_1, \ldots, D_4$ to create an updated D.
- Update C by the least squares technique on the fictitious MIMO problem.

Several iterations of this procedure were used to generate the four-input, three-output model used for control design.

The identified MIMO model resulted from the above approach shows satisfactory results overall. However, some elements of transfer functions have much better match with the measured data (Figure 14) than the other (Figure 15).

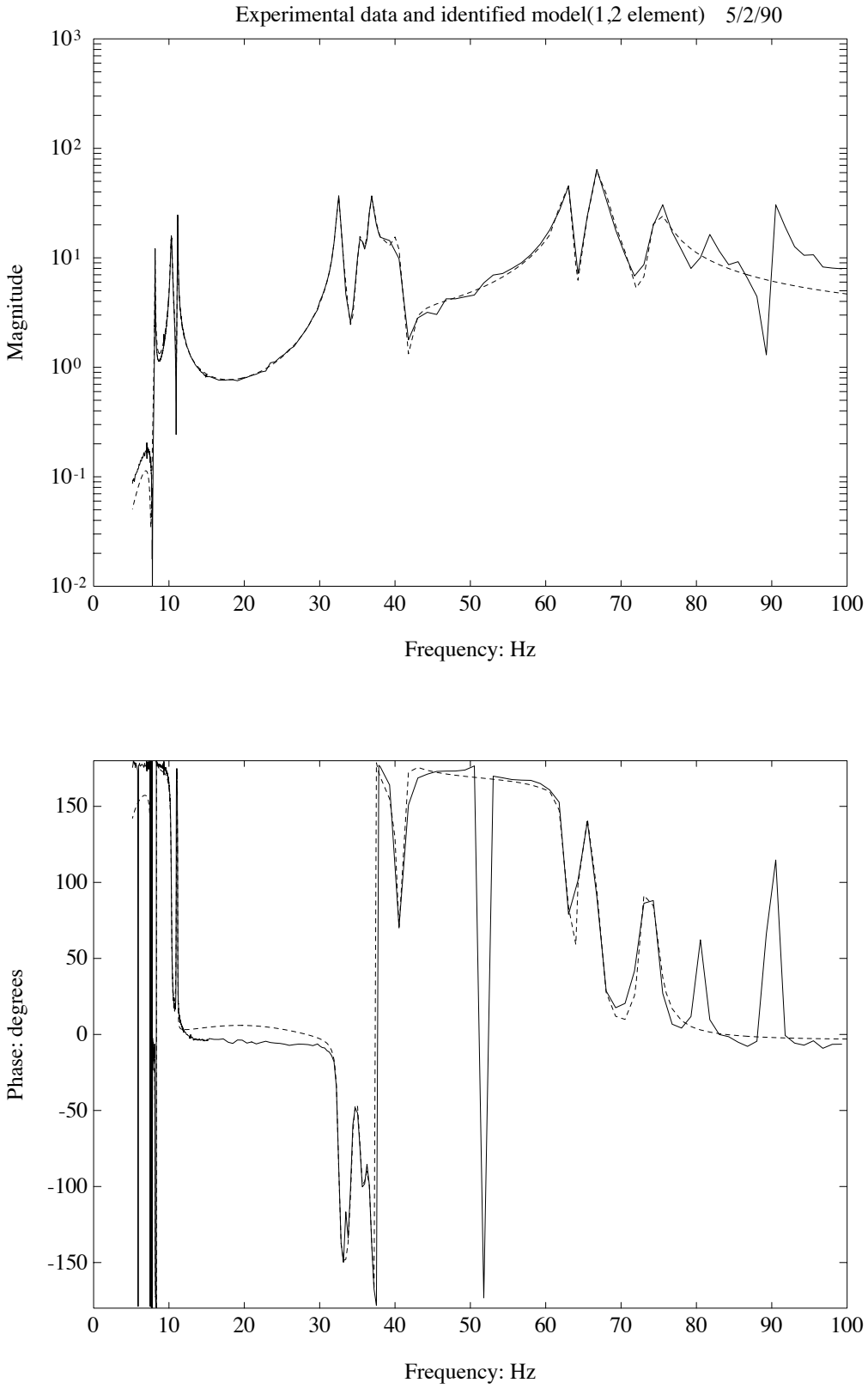

Figure 14: Frequency Response: $S_{1,2}$ (solid line) and $M_{1,2}$ (dashed line)

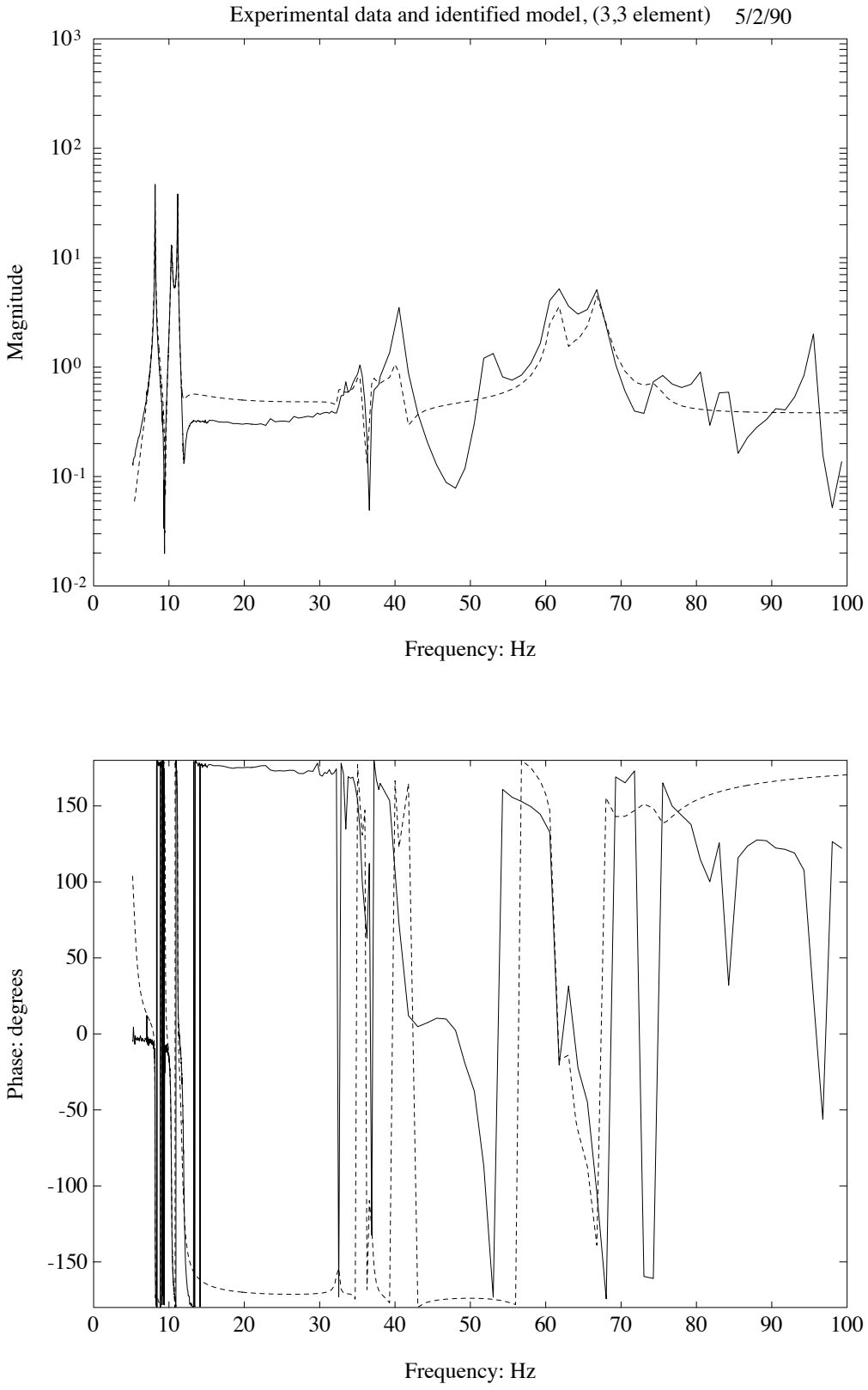

Figure 15: Frequency Response: $S_{3,3}$ (solid line) and $M_{3,3}$ (dashed line)

Conclusions

Our work has demonstrated that collocated control on active members is an effective means of achieving high levels of damping in truss structures. Minimal knowledge of the plant drive point impedances is required to achieve good impedance matches even with relatively simple force feedback techniques. The dial-a-strut implementation of the bridge feedback method makes the impedance matching task particularly straightforward. The noncollocated robust control approaches are complex to implement, but do produce controllers with good performance. It is very important to have an accurate multi-input-output model for this design paradigm. Our ad-hoc approach to the identification problem has given mixed results. There is a strong need for improved identification methods, particularly for more heavily damped structures.

We have found that added passive damping in the lower modes did not significantly improve closed loop performance. We expect that damping in the higher frequency modes will result in higher available loop gain that will in turn enable higher performance. This will be a topic of future research. Our single test of robust performance showed that a controller designed for a damped structure still performed well when the damping of the structure was reduced a factor of ten. Further robustness tests involving modal frequencies are planned for future work. Finally, the selection of weights for the robust controllers has been somewhat arbitrary. We feel that scaling these weights to more physically motivated values will achieve improved performance. The parameterization of uncertainty is also very crude in our designs, improved methods using modal parameters may lead to superior performance and is a good topic for future work.

Acknowledgments

The authors wish to acknowledge the contributions of Dr. Clark Briggs for the design of the HUGH 9000, Dr. Dankai Liu for software and for conducting the digital closed loop experiments, and Mr. John O'Brien for fabrication of the dial-a-strut controllers and for conducting the active damping tests. The research described in this paper was carried out by the Jet Propulsion Laboratory, California Institute of Technology, under a contract with the National Aeronautics and Space Administration.

References

[1] R.A. Laskin and M. San Martin. "Control/Structure System Design of a Spaceborne Optical Interferometer". In *Proceedings of the AAS/AIAA Astrodynamics Specialist Conference, Stowe, VT*, 1989.

[2] J.L. Fanson and J.A. Garba. "Experimental Studies of Active Members in Control of Large Space Structures". In *Proceedings of the 29th AIAA SDM Conference, Williamsburg, VA*, pages 9–17, 1988.

[3] J.L. Fanson, C-C. Chu, R.S. Smith, and E.H. Anderson. "Active Member Control of a Precision Structure with an H_∞ Performance Objective". In *Proceedings of the AIAA Dynamics Specialists Conference, Long Beach, CA*, pages 322–333, 1990.

[4] M. Morari and E. Zafiriou. *Robust Process Control*. Englewood Cliffs: Prentice-Hall Inc., 1989.

[5] G-S. Chen and B.J. Lurie. "Bridge Feedback for Active Damping Augmentation". In *Proceedings of the AIAA Dynamics Specialists Conference, Long Beach, CA*, pages 502–509, 1990.

[6] H.C. Briggs. "JPL Control/Structure Interaction Test Bed Real-Time Control Computer Architecture". In *Proceedings of the 3rd Annual Conference on Aerospace Computational Control, Oxnard, CA*, pages 739–755, 1989.

[7] R.S Smith. *Procedures for the Identification of the Precision Truss*. Technical Report JPL D-7791, Jet Propulsion Laboratory, 1990.